Role of fluctuations in a thermal phase transition in a nucleus probed via the giant dipole resonance

Deepak Pandit,[1,*] Srijit Bhattacharya,[2] Debasish Mondal,[1] Balaram Dey,[3] S. Mukhopadhyay,[1,4] Surajit Pal,[1] A. De,[5] and S. R. Banerjee[6]

[1]*Variable Energy Cyclotron Centre, 1/AF-Bidhannagar, Kolkata 700064, India*
[2]*Department of Physics, Barasat Govt. College, Barasat, N 24 Pgs, Kolkata 700124, India*
[3]*Saha Institute of Nuclear Physics, 1/AF-Bidhannagar, Kolkata 700064, India*
[4]*Homi Bhabha National Institute, Training School Complex, Anushaktinagar, Mumbai 400094, India*
[5]*Department of Physics, Raniganj Girls' College, Raniganj 713358, India*
[6]*(Ex)Variable Energy Cyclotron Centre, 1/AF-Bidhannagar, Kolkata 700064, India*

(Received 6 November 2018; revised manuscript received 9 January 2019; published 19 February 2019)

We present an experimental investigation of thermal phase transition in atomic nuclei by measuring the γ rays from the decay of the giant dipole resonance in ^{169}Tm populated by using the reaction ^{4}He + ^{165}Ho. The systematic measurement confirms the prolate shape, similar to the ground-state value, till temperature $T = 1.23$ MeV. Moreover, the present data, together with the previous experimental studies, point towards the persistence of prolate shape with deformation similar to that of the ground state till $T = 1.5$ MeV. In addition, the emergence and evolution of thermal fluctuations observed directly in the experiment suggest that the sharp phase transition from prolate to near spherical at $T \approx 1.7$ MeV will not be evident experimentally due to statistical fluctuations owing to the finite size of the nucleus.

DOI: 10.1103/PhysRevC.99.024315

I. INTRODUCTION

The study of finite quantal systems is very fascinating as they possess the properties of both microscopic (separate quantum particles) and macroscopic sizes (large statistical systems). It is remarkable that finite systems having different physical nature can exhibit similar physical features [1]. For example, the shell effects, caused by the degeneracy of quantum spectra, exist in quantum dots, atomic nuclei, and metallic grains. In atomic nuclei, the shell effect creates small fluctuations in the total potential energy obtained from the liquid drop model [2]. Although, amounting to only about 1% of the total binding energy, it governs the variation of ground-state nuclear shapes along isotopic and isotonic chains [3], and is one of the driving effects in the production of superheavy elements [4]. When a shell is completely filled, it leads to strong shell effects manifested by the stability of the nuclei. However, when the shell is only partially filled, it breaks the spherical symmetry and the residual interactions among the valence nucleons drag the nucleus to a deformed ground state.

The quantum phase transition, an abrupt change in the state of a many-body system at zero temperature ($T = 0$) [5], is connected with the nuclear shape transition from spherical to deformed or from axially deformed to nonaxially deformed shapes [6]. Interestingly, the ground-state deformation of the nuclei, arising due to shell effects, can also be altered by increasing the excitation energy. The thermal excitations weaken the shell effects and act in the direction of decreasing the equilibrium deformation leading to a thermal phase transition from deformed to spherical shape [7]. Along with shape transition, the idea of phase transition in nuclear physics also involves vanishing of pairing correlations at excitation energies above a few MeV (superfluid to normal fluid transition), nuclear multifragmentation in the Fermi energy domain (liquid to gas phase transition), and deconfined state of quark-gluon-plasma in the ultrarelativistic region. However, it should be emphasized that in small finite systems at finite T, the thermal fluctuations are expected to be large and could play a decisive role in defining the properties of the system, particularly in the phase-transition region. For example, the studies of fluctuation on pairing effect have shown that the sharp phase transition from superfluid to normal fluid is effectively washed out [8–10]. The theoretical calculations, based on the mean-field theory for nuclear shape transition, often predict sharp phase transitions at finite temperature [11–14]. Intriguingly, when the effect of shape fluctuations is taken into account, it suggests a substantial smearing of the transition [15,16]. In this scenario, whether the T-driven phase transition will be evident experimentally still remains an open question.

One of the experimental probes to study the shapes and fluctuations of hot nuclei is the giant dipole resonance (GDR) [17–19]. It can be interpreted as the out-of-phase oscillation of the proton fluid against the neutron fluid and its cross section is characterized by a Lorentzian function having a strength (S_{GDR}), a centroid energy (E_{GDR}), and a width (Γ_{GDR}). The GDR strongly couples with the nuclear shape degrees of freedom. Hence, in the case of deformed nucleus, the GDR strength splits into different components with frequencies inversely proportional to the lengths of the principal axes, providing a direct information about the

*deepak.pandit@vecc.gov.in

nuclear deformation [18]. The hydrodynamical model predicts the ratio $S_{GDR2}/S_{GDR1} \approx 2$ for a prolate nucleus, and $\approx$0.5 for an oblate nucleus [17]. A few experimental attempts have been made earlier to probe the T-driven shape transitions, by using the GDR in the rare-earth region, but the results have been conflicting as the shape of the nuclei could not be uniquely determined [20–23].

In this paper, our aim is to show the actual shape of the excited nucleus in rare-earth region by using α-induced fusion reactions, which allow probing the shape independent of angular momentum (J)-driven effects. By performing systematic investigation and comparing with the previous experimental results, the shape of the nucleus has been extracted up to $T = 1.5$ MeV, which removes the conflict in the existing literatures regarding the nature of the ellipsoid (prolate/oblate). Moreover, since the fluctuation is observed directly in the experiment it provides a unique opportunity to study the emergence and evolution of thermal fluctuations in small finite systems.

II. EXPERIMENTAL DETAILS AND ANALYSIS

The ^{169}Tm compound nucleus was populated through the reaction ^{4}He + ^{165}Ho at four beam energies 32, 37, 42, and 50 MeV by using the K-130 room-temperature cyclotron at VECC. The critical angular momentum for fusion at the highest beam energy was 21 $\hbar$. The high-energy GDR γ rays were detected at 90° and 125° angles with respect to the incident beam direction by employing the LAMBDA spectrometer [24,25], arranged in a 7 × 7 matrix, at a distance of 50 cm from the target position. Though the angular momentum populated in the above reactions does not affect the GDR parameters ($J_c = 43\hbar$ for ^{169}Tm [26]), determination of J is crucial for a precise evaluation of nuclear temperature. Therefore, the 50-element low-energy γ multiplicity filter [27] was used to estimate the angular momentum populated in the compound nucleus. The filter was split into two blocks of 25 detectors each and was placed on the top and the bottom of the scattering chamber at a distance of 5 cm from the target center. A master trigger was generated when at least one detector each from the top and bottom blocks fired together in coincidence with a high-energy γ ray($\geqslant$5 MeV) measured in any of the large detectors in the LAMBDA array. This ensured the selection of high-energy photons from the higher part of the CN spin distribution and considerably reduced the background. The neutron and the pileup events in LAMBDA were rejected by time-of-flight and pulse shape discrimination techniques, respectively. The cyclotron rf time spectrum was also recorded with respect to the master trigger to ensure the selection of beam-related events. The details of the GDR analysis have already been discussed in our earlier papers [28–31].

The γ-ray spectra from the decay of ^{169}Tm nucleus at initial excitation energies of 30.0, 34.9, 39.8, and 47.6 MeV are displayed in Fig. 1. They show the typical broad bump of the GDR beyond 9 MeV where the spectrum changes from the exponentially decreasing characteristics of the low-energy statistical transitions. Most noteworthy is the two components of the GDR (around 12 and 16 MeV) directly visible in the high-energy spectrum at 32 MeV beam energy

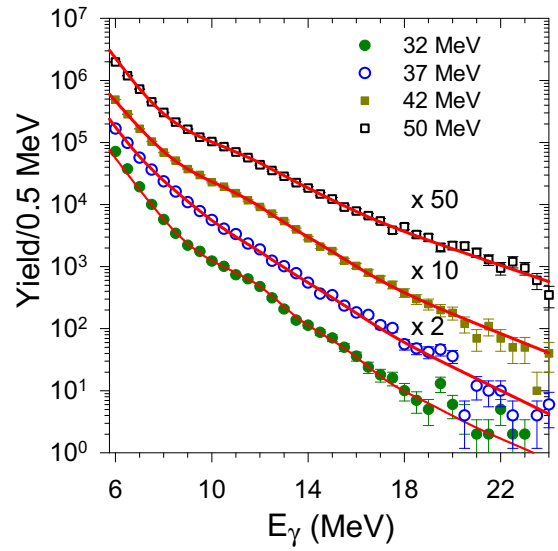

FIG. 1. The experimental γ spectra measured at 90° angle at different beam energies are compared with the results of the statistical model calculations plus a bremsstrahlung component (continuous lines).

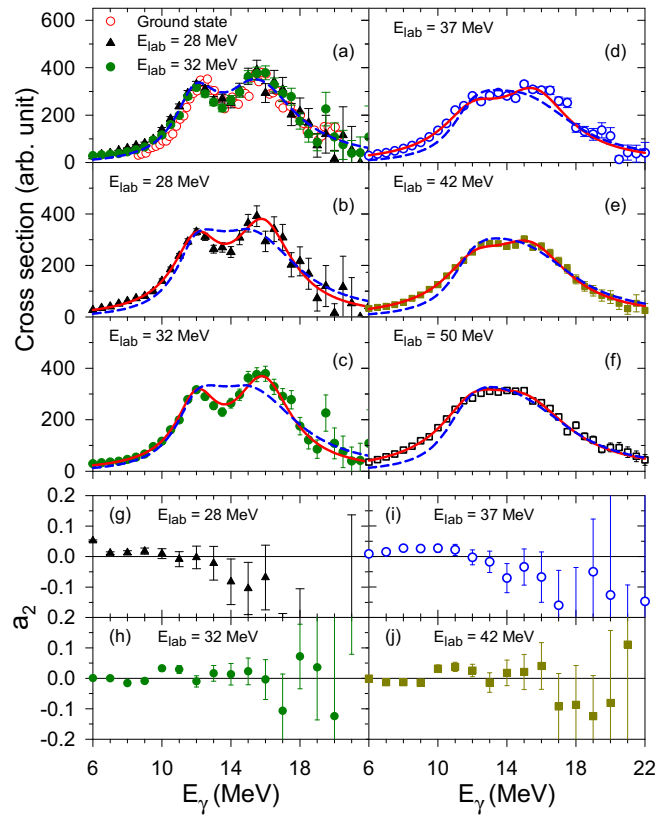

FIG. 2. The linearized GDR strength functions at different beam energies [(a)–(f)]. The solid lines are $F(E_\gamma)$ used in the CASCADE calculation. The dashed lines represent the TSFM calculations. The TSFM calculation at $T = 0.2$ MeV is compared with the ground-state value in (a). The angular anisotropy coefficients at different beam energies are shown in (g)–(j).

TABLE I. Extracted GDR parameters at different beam energies.

E_{lab} (MeV)	$\langle T\rangle$ (MeV)	$\langle J\rangle$ $\hbar$	E_{GDR1} (MeV)	Γ_{GDR1} (MeV)	E_{GDR2} (MeV)	Γ_{GDR2} (MeV)	$\frac{S_{GDR2}}{S_{GDR1}}$
28	0.75 ± 0.05	12 ± 4	12.1 ± 0.4	3.3 ± 0.6	16.0 ± 0.5	4.1 ± 0.7	2.4 ± 0.3
32	0.85 ± 0.05	14 ± 4	12.2 ± 0.4	2.9 ± 0.4	16.0 ± 0.5	4.0 ± 0.5	2.5 ± 0.3
37	0.95 ± 0.05	16 ± 4	12.2 ± 0.4	4.3 ± 0.4	15.8 ± 0.6	5.0 ± 0.5	2.3 ± 0.3
42	1.05 ± 0.05	18 ± 5	12.3 ± 0.4	4.3 ± 0.5	15.6 ± 0.5	5.6 ± 0.6	2.6 ± 0.4
50	1.23 ± 0.05	20 ± 5	12.2 ± 0.3	4.5 ± 0.5	15.4 ± 0.4	6.4 ± 0.7	2.3 ± 0.3

indicating a large deformation independent of any model. The GDR parameters at different beam energies were obtained by comparing the experimental data with the results of the statistical model calculations performed by using a modified version of the CASCADE code [32,33], along with a bremsstrahlung component parametrized as $\sigma = \sigma_0 e^{-E_\gamma/E_0}$, folded with the detector response function. The slope parameter (E_0) was chosen according to the bremsstrahlung systematic [34], which has been verified in our previous experiments [30,35]. The measured fold distributions were mapped onto the angular momentum space by using a realistic technique based on GEANT simulation [27] and used as inputs for the statistical model calculation. Recently, the collective enhancement effect on the nuclear level density (NLD) was studied in the same reaction at two beam energies of 28 and 40 MeV [36,37]. Hence, the same enhanced NLDs, deformation parameters, Ignatyuk prescription of level density parameter [38] with asymptotic NLD parameter ($A/8$) and transmission coefficients were used in the statistical model calculation at all the beam energies. The linearized GDR plots along with the best-fit CASCADE spectra are shown in Fig. 2 by using the quantity $F(E_\gamma)Y^{exp}(E_\gamma)/Y^{cas}(E_\gamma)$, where, $Y^{exp}(E_\gamma)$ and $Y^{cas}(E_\gamma)$ are the experimental and the best-fit CASCADE spectra, respectively, corresponding to the two-component Lorentzian function $F(E_\gamma)$. The extracted GDR parameters at different beam energies are given in Table I. The uncertainties were obtained by χ^2 minimization procedure in the energy range 8–20 MeV.

III. RESULT AND DISCUSSION

The experimentally determined absorption cross section at 32 MeV are compared with the available ground-state photoabsorption cross section for ^{170}Yb [39] (similar prolate ground-state deformation as ^{169}Tm) along with our earlier data at 28 MeV [36] in Fig. 2(a). The data at 28 and 32 MeV are in very good agreement with the ground-state photoabsorption cross section in this mass region [39,40] confirming that the shape of the nucleus at these excitation energies is indeed prolate, with roughly the same ground-state deformation. Our result supports the predictions of the Brink-Axel hypothesis. We emphasize here that the spectra, at all the beam energies, could not be explained considering a single Lorentzian. The data at 32, 37, and 42 MeV could only be explained considering photoabsorption cross section corresponding to prolate shapes in the statistical model calculation. On the other hand, an equally good fit was obtained considering both prolate and oblate shapes for 50 MeV data. The result is similar to the previous studies on ^{166}Er, which suggested both oblate deformation [20] and prolate deformation [21] at somewhat similar T. A later study on ^{160}Er also produced similar results [22]. However, in all the cases, one-component GDR fits were inadequate and the oblate solution was obtained having $\Gamma_{GDR1} > \Gamma_{GDR2}$, which is contrary to the experimentally observed values and hydrodynamic considerations [41].

The shape of the GDR in deformed nuclei may be quantitatively related to the nuclear deformation by using the hydrodynamic model [42]. Considering an ellipsoid shape, the experimental deformation can be calculated from the relation $\beta_{exp} = \sqrt{\frac{4\pi}{5}}\frac{d-1.0}{0.5d+0.87}$, where d is the ratio of the two GDR components (E_{GDR2}/E_{GDR1}), related to the ratio of the half-axes of axially symmetric deformed nucleus [22]. The extracted deformations from the two GDR components at different $\langle T\rangle$ are shown in Fig. 3(a). The average temperature of the compound nucleus associated with the GDR decay was estimated from $\langle T\rangle = [(\overline{E}^* - \overline{E}_{rot} - E_{GDR} - \Delta_p)/a(\overline{E}^*)]^{1/2}$,

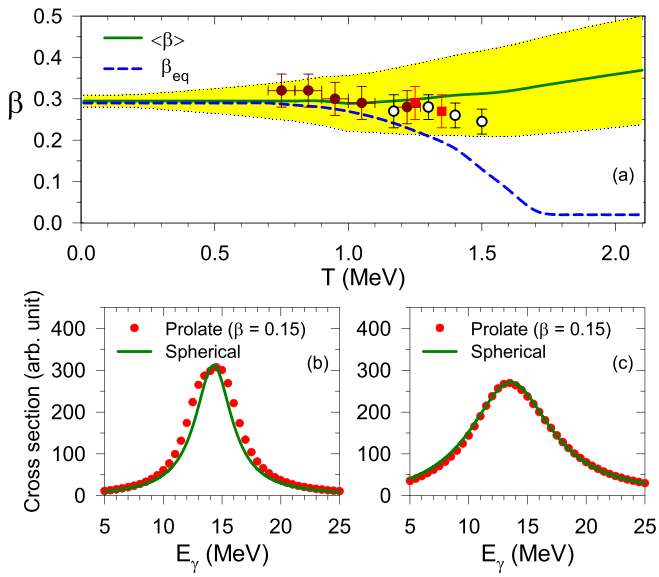

FIG. 3. (a) The extracted experimental deformations for ^{169}Tm (filled circles), ^{160}Er [21,22] (open circles) and ^{166}Er [20,21] (filled square) are compared with the theoretical deformations. The shaded region corresponds to the standard deviation. The GDR spectral shape for prolate deformation ($\beta = 0.15$) and spherical shape are compared with each other by not considering (b) and considering (c) thermal fluctuations.

where $\overline{E^*}$ is the average of the excitation energy weighed over the daughter nuclei for the γ emission in the GDR region. Δ_p is the pairing energy and $\overline{E}_{\rm rot}$ is the rotational energy computed at average $\langle J\rangle$ within the CASCADE corresponding to selected fold distribution [32]. However, at these excitation energies, the GDR decay is predominantly from the initial stages and the averaging only reduces the average temperature by ≈8% at the highest beam energy. It is very interesting to find that the shape and magnitude of deformation at these excitations are unchanged from the values known from the ground-state photoabsorption in this mass region. The deformations extracted for ^{166}Er and ^{160}Er in the previous experiments at higher T [20–22] are also compared with the present data. The prolate ground-state deformation of ^{166}Er and ^{160}Er are 0.28 and 0.25, respectively [3]. The temperatures of Refs. [20,21] have been reestimated by averaging over the decay steps, while the average temperature quoted in Ref. [22] have been used directly, in order to bring all the data on the same footing. It is intriguing to find that the extracted deformations even at $T = 1.5$ MeV are very similar to the ground-state values. Since we could uniquely determine the shape of the nucleus as prolate, the shapes of ^{166}Er and ^{160}Er at slightly higher T can also be believed to be prolate. Although the shapes were not sharply defined, it seems improbable for nuclear shape to change from prolate to oblate with similar magnitude of deformation with only slight change in T(≈0.3 MeV). The angular anisotropy coefficients were also measured at 32, 37, and 42 MeV beam energies and are shown in Figs. 2(g)–2(j). They were identical at all the energies and very small (2–3 %) even though the extracted deformations are large and similar to the equilibrium values. The attenuation of the measured angular anisotropy is probably due to the large effects of the orientation fluctuations at smaller angular frequency ($\omega \approx 0.2$ MeV selected in the experiment) [23,43].

In order to illustrate the shape transition and deformation expected in this mass region, the free energy for ^{169}Tm as a function of the intrinsic quadrupole deformation coordinates β, γ at $J = 20\hbar$ are shown in Fig. 4. The free energy $F(T, J, \beta, \gamma)$ was calculated considering the deformed liquid drop energy, Strutiusky shell corrections, entropy, and rotational energy following the prescription in Refs. [44–48]. The single-particle energies (e_i) were calculated by using the deformed Woods-Saxon potential with the universal parameters [49] and the entropy was estimated by using the relation $S = -\sum_i f_i \cdot \ln(f_i) - \sum_i (1 - f_i) \cdot \ln(1 - f_i)$, where $f_i = [1 + \exp\{(e_i - \mu)/T\}]^{-1}$ is the Fermi occupation numbers with μ as the chemical potential. The calculated equilibrium shape of ^{169}Tm is prolate ($\beta = 0.29$) at $T = 0$ and the increase of T induces a shape transition from prolate to near spherical (slight oblate $\beta = 0.03$ for finite $J = 20\hbar$) at $T =$ 1.7 MeV. The evolution of equilibrium deformation ($\beta_{\rm eq}$) with T is compared with the experimental data in Fig. 3(a). From the trend of experimental data, it appears very unlikely that the shape phase transition will occur at $T \approx 1.7$ MeV because of the large magnitude and the small change of β with T.

Since nucleus is a small finite system, statistical fluctuations are expected to be large. It is highly interesting to note that the effect of fluctuation is seen directly in the experimental data (Fig. 2). The two GDR peaks are clearly separated

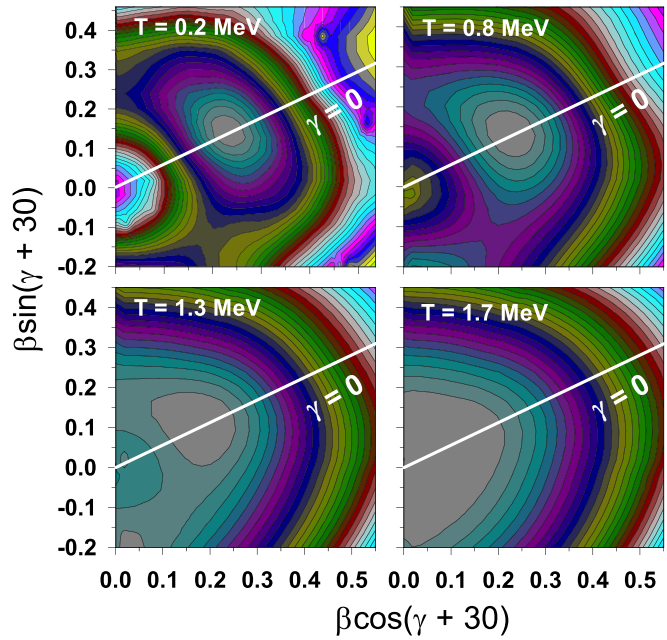

FIG. 4. Free energy surfaces at different T and $J = 20\hbar$ for ^{169}Tm. The y axis corresponds to the oblate shape while the thick solid line represents the prolate shape ($\gamma = 0$).

below $T = 0.9$ MeV. Above $T \approx 1$ MeV, the two peaks start to become broader due to the averaging effect of thermal fluctuations and finally get convoluted at $T \approx 1.2$ MeV but the ratio $E_{\rm GDR2}/E_{\rm GDR1}$ remains almost unchanged, which unambiguously determines the deformation. The data have also been compared with the thermal shape fluctuation model calculations in which the GDR vibration is averaged over the free energy surfaces by using the Boltzmann probability $e^{-F/T}$ with the volume element $\beta^4 \sin(3\gamma) d\beta d\gamma$ [44,45]. In general, the calculations are in good agreement with the data highlighting that the shape of the nucleus is indeed prolate and the GDR spectrum is highly convoluted at higher T due to the thermal shape fluctuations. It is also remarkable to observe that the experimental GDR line shapes show no signature of thermal fluctuations below $T = 0.9$ MeV and provide an unique platform to check the existing models [50,51].

In order to study the effect of fluctuations on the equilibrium shape, the average deformation $\langle\beta\rangle$ and the standard deviation $\Delta\beta = [\langle\beta^2\rangle - \langle\beta\rangle^2]^{1/2}$ were also estimated following the prescription described in Ref. [52] and are shown in Fig. 3(a). It is very interesting to note that $\langle\beta\rangle$ is very similar to the equilibrium deformation up to $T = 0.8$ MeV but deviates significantly beyond $T \approx 1.0$ MeV. The average shape produced by the fluctuations does not pass through the shape phase transition. It is also important to note the associated standard deviation becomes larger at higher T, complicating the GDR spectral shape. Therefore, it becomes experimentally difficult to draw a conclusion on the shape of the nucleus. As a result, it appears that the shape transition from prolate to near spherical will not be observed experimentally at higher T since, in the midst of large thermal shape fluctuations, the GDR spectral shape of prolate deformation with $\beta = 0.15$ will effectively be the same as a spherical

nucleus as shown in Fig. 3(c). Our results could throw some light on the study of phase transitions under the constraint of small finite systems, e.g., the pairing phase transition not seen directly in the neutron evaporation spectrum, smoothening of the caloric curve in liquid-gas phase transition, and T-driven phase transition in two-dimensional graphene [53]. Besides, our work may be relevant regarding the hitherto observed experimental evidences of antiferromagnetism in the unconventional superconductors [54].

IV. CONCLUSION

In summary, the present work emphasizes that the shape of the nuclei in rare-earth region remains prolate with deformation remarkably similar to the ground-state value till $T = 1.5$ MeV. However, the shape fluctuations about the equilibrium shape are quite large at higher T, observed directly in the present study, which indicates that the sharp phase transition from prolate to near spherical predicted to occur at $T \approx 1.7$ MeV will not be evident experimentally.

ACKNOWLEDGMENTS

The authors are thankful to VECC cyclotron operators for smooth running of the accelerator during the experiments. B.D. would like to thank SERB, DST, Government of India for financial support of the national postdoctoral fellowship (PDF/2017/000246).

[1] J. L. Birmana, R. G. Nazmitdinov, and V. I. Yukalov, Phys. Rep. **526**, 1 (2013).
[2] A. Bohr, B. R. Mottelson, *Nuclear Structure* (Benjamin, New York, 1969), Vols. 1, 2.
[3] P. Moller *et al.*, At. Data Nucl. Data Tables **59**, 185 (1995).
[4] F. P. Heßerger, Chem. Phys. Chem. **14**, 483 (2013).
[5] M. Vojta, Rep. Prog. Phys. **66**, 2069 (2003).
[6] R. F. Casten, Nature Phys. **2**, 811 (2006).
[7] J. L. Egido, L. M. Robledo, and V. Martin, Phys. Rev. Lett. **85**, 26 (2000).
[8] L. G. Moretto, Phys. Lett. B **40**, 1 (1972).
[9] A. L. Goodman, Phys. Rev. C **29**, 1887 (1984).
[10] N. D. Dang and A. Arima, Phys. Rev. C **68**, 044303 (2003).
[11] Y. Alhassid, J. M. Manoyan, and S. Levit, Phys. Rev. Lett **63**, 31 (1989).
[12] B. K. Agrawal, Tapas Sil, S. K. Samaddar, and J. N. De, Phys. Rev. C **63**, 024002 (2001).
[13] A. L. Goodman and T. Jin, Phys. Rev. C **54**, 1165 (1996).
[14] W. Zhang and Y. F. Niu, Phys. Rev. C **97**, 054302 (2018).
[15] J. L. Egido, C. Dorso, J. O. Rasmussen, and P. Ring, Phys. Lett. B **178**, 139 (1986).
[16] A. L. Goodman, Phys. Rev. C **37**, 2162 (1988).
[17] M. N. Harakeh and A. van der Woude, *Giant Resonances, Fundamental High-frequency Modes of Nuclear Excitation* (Clarendon Press, Oxford, 2001).
[18] J. J. Gaardhøje, Ann. Rev. Nucl. Part. Sci. **42**, 483 (1992).
[19] D. R. Chakrabarty, N. Dinh Dang, and V. M. Datar, Eur. Phys. J. A **52**, 143 (2016).
[20] J. J. Gaardhoje, C. Ellegaard, B. Herskind, and S. G. Steadman, Phys. Rev. Lett. **53**, 148 (1984).
[21] C. A. Gossett, K. A. Snover, J. A. Behr, G. Feldman, and J. L. Osborne, Phys. Rev. Lett. **54**, 1486 (1985).
[22] D. R. Chakrabarty, M. Thoennessen, S. Sen, P. Paul, R. Butsch, and M. G. Herman, Phys. Rev. C **37**, 1437 (1988).
[23] F. Camera *et al.*, Nucl. Phys. A **572**, 401 (1994).
[24] S. Mukhopadhyay *et al.*, Nucl. Instr. Meth. A **582**, 603 (2007).
[25] Balaram Dey *et al.*, Nucl. Instr. and Meth. A **727**, 7 (2013).
[26] D. Kusnezov, Y. Alhassid, and K. A. Snover, Phys. Rev. Lett. **81**, 542 (1998).
[27] D. Pandit *et al.*, Nucl. Instr. and Meth. A **624**, 148 (2010).
[28] D. Pandit *et al.*, Phys. Lett. B **690**, 473 (2010).
[29] D. Pandit *et al.*, Phys. Lett. B **713**, 434 (2012).
[30] Balaram Dey *et al.*, Phys. Lett. B **731**, 92 (2014).
[31] D. Mondal *et al.*, Phys. Rev. Lett. **118**, 192501 (2017).
[32] S. Bhattacharya *et al.*, Phys. Rev. C **78**, 064601 (2008).
[33] S. Bhattacharya *et al.*, Phys. Rev. C **90**, 054319 (2014).
[34] H. Nifennecker and J. A. Pinston, Annu. Rev. Nucl. Part. Sci. **40**, 113 (1990).
[35] D. Mondal *et al.*, Phys. Lett. B **784**, 423 (2018).
[36] D. Pandit *et al.*, Phys. Rev. C **97**, 041301(R) (2018).
[37] P. Roy *et al.*, Phys. Rev. C **88**, 031601(R) (2013).
[38] A. V. Ignatyuk, G. N. Smirenkin, and A. S. Tishin, Sov. J. Nucl. Phys. **21**, 255 (1975) [Yad. Fiz. **21**, 485 (1975)].
[39] A. V. Varlamov, V. V. Varlamov, D. S. Rudenko, and M. E. Stepanov, Atlas of Giant Dipole Resonances, INDC(NDS)-394, 1999 (unpublished); JANIS database.
[40] B. L. Berman and S. C. Fultz, Rev. Mod. Phys. **47**, 713 (1975).
[41] A. R. Junghans *et al.*, Phys. Lett. B **670**, 200 (2008).
[42] M. Danos, Nucl. Phys. **5**, 23 (1958).
[43] A. Maj *et al.*, Nucl. Phys. A **571**, 185 (1994).
[44] Y. Alhassid and B. Bush, Phys. Rev. Lett. **65**, 2527 (1990).
[45] P. Arumugam, G. Shanmugam, and S. K. Patra, Phys. Rev. C **69**, 054313 (2004).
[46] N. Dubray, J. Dudek, and A. Maj, Acta Physica Polonica B **36**, 1161 (2005).
[47] D. Pandit, S. Mukhopadhyay, S. Bhattacharya, S. Pal, A. De, S. Bhattacharya, C. Bhattacharya, K. Banerjee, S. Kundu, T. K. Rana, A. Dey, G. Mukherjee, T. Ghosh, D. Gupta, and S. R. Banerjee, Phys. Rev. C **81**, 061302(R) (2010).
[48] D. Pandit *et al.*, Phys. Rev. C **95**, 034301 (2017).
[49] S. Cwiok *et al.*, Comput. Phys. Commun. **46**, 379 (1987).
[50] A. K. Rhine Kumar, P. Arumugam, and N. D. Dang, Phys. Rev. C **90**, 044308 (2014).
[51] N. D. Dang and N. Q. Hung, Phys. Rev. C **86**, 044333 (2012).
[52] D. Pandit *et al.*, Phys. Rev. C **87**, 044325 (2013).
[53] V. M. Loktev and V. Turkowski, Phys. Rev. B **79**, 233402 (2009).
[54] B. Keimer *et al.*, Nature (London) **518**, 179 (2015).